Ultraviolet Laser Oscillations of Multiple Ionized Ions in Z-Pinch Discharge

AUTHOR(S):

HASHINO, Yasuo; KATSUYAMA, Yutaka; FUKUDA, Kuniya

CITATION:

HASHINO, Yasuo ...[et al]. Ultraviolet Laser Oscillations of Multiple Ionized Ions in Z-Pinch Discharge. Memoirs of the Faculty of Engineering, Kyoto University 1974, 36(3): 213-234

ISSUE DATE:

1974-10-31

URL:

http://hdl.handle.net/2433/280948

Ultraviolet Laser Oscillations of Multiple Ionized Ions in Z-Pinch Discharge

By

Yasuo HASHINO*, Yutaka KATSUYAMA** and Kuniya FUKUDA***

(Received March 29, 1974)

Abstract

Pulse laser oscillations from multiple ionized N, O and rare gases were observed in the ultraviolet region for the Z-pinch discharge. Optimum value of gas pressure, oscillation time and its pressure dependence were examined for laser oscillations. It has been found that oscillations from different ions occur in the increasing order of ionization after the breakdown of discharge. The line ArII λ4765 A showed an anomalous behavior. Calculation is made on two different models for ionization and excitation of plasma. The first one is concerned with ionization and excitation by thermal electrons during plasma compression. The second one is concerned with direct excitation of laser oscillation by runaway electrons. The calculation based on the former explains the temporal sequence of laser oscillations; and that on the latter explains the anomalous behavior of ArII λ4765 A line.

1. Introduction

W. R. Bennett[1] first discussed the pinch effect in the pulse ion laser and pointed out that the fluctuation of the laser output of ArII λ5145A synchronized with the current noise due to the pinch effect in a quasi cw-oscillation. He also demonstrated the influence of high speed electrons produced from the instability of the pinch plasma on the laser output. These phenomena were called "plasma interaction" in the pulse discharge of the ion laser in a capillary. Since then, the plasma interaction has been treated only incidentally in some papers on the pulse ion laser.[2~4]

On the other hand, the effect of a transient high current pinch discharge such as θ- or linear Z-pinch has been scarcely discussed in connection with laser oscillation.

* Department of Mechanical Engineering II. The Fellowship of Japan Society for the Promotion of Science for the period from April 1973 to March 1975.
** Department of Mechanical Engineering II. Present address: Ibaraki Annex of the Electrical Communication Lab., Nippon Telegraph and Telephone Public Corporation, Ibaraki.
*** Department of Mechanical Engineering II

Laser oscillation by means of Z-pinch effect was first recorded as ArII λ4765A[5,6], later as ArII λ3511 and 3638A[7], and then as several Xe ion lines.[8] A detailed experiment has followed to observe the temporal profiles of oscillation pulse and plasma parameters.[9,10] In the θ-pinch discharge, the laser oscillation has been recorded as NI λ4321 and 4329A.[11]

In the high current pinch discharge a larger amount of energy is fed in a much shorter period, compared with the usual pulse discharge of the ion laser in a capillary.[2,12,13] Hence, an effective compression of plasma takes place to give rise to highly ionized plasma at a high temperature. This fact gives promise of the high output power of the pulse laser oscillation from highly ionized species, and hence, of the oscillation at a very short wavelength in the ultraviolet or vacuum ultraviolet region.

In the present work, the laser oscillations from multiple ionized ions have been examined in the ultraviolet region for the Z-pinch discharge of the rare gases, O_2 and N_2. In the next section, the experimental procedures are introduced, and in §3, the results of the experiment are presented. In §4, the calculation is made on the two simple models of ionization and excitation processes in the Z-pinch discharge, *i.e.*, the ionization by thermal electrons during the plasma compression and the direct excitation by runaway electrons for the laser oscillations. In the last section, the observed behaviors of the laser oscillation lines from the multiple ionized ions are discussed in relation to the results of the calculations.

2. Experiment

The experiment was performed with two kinds of apparatus, (*A*)[14] and (*B*).[15] Fig. 1 shows the experimental set-up of apparatus (*A*). The Z-pinch laser tube consists of a pyrex tube of 20 mm diameter, a return conductor, two copper electodes set at a distance 1 m and the internal mirror system of an optical resonator. The resonator is formed by two Al-coated mirrors (R=1 or 2 m), the front one of which has a pinhole of 0.5 mm diameter in its center to pass the laser light. The mirror holders were connected to the discharge tube by means of O-ring seals, which made it easy to exchange the mirrors. Before a series of experiments, the Al-coated mirrors were put into the mirror holders soon after the evaporation of the Al-layer. The vacuum system, including the mirror holders and the discharge tube, was evacuated and kept at about 10^{-5} Torr so that the development of an Al_2O_3 layer was prevented. In apparatus (*B*), the discharge tube was the same as that of (*A*), but it had Brewster windows. The external mirror system of an optical resonator consisted of the same mirrors as those of (*A*), but sometimes the front mirror was replaced by a dielectric-coated mirror so that the power from some specific laser oscillation could be measured in the visible region.

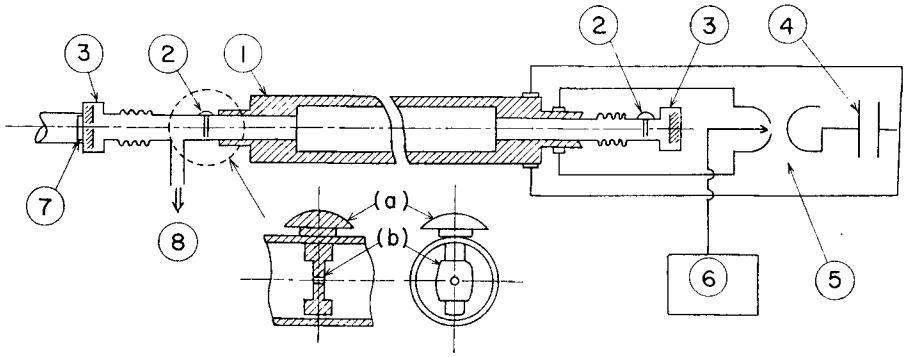

Fig. 1. The experimental set-up of the apparatus (*A*). 1: discharge tube, 2: magnetic pin (a) and magnetically movable diaphragm with a pinhole (b), 3: mirror and mirror holder, 4: condenser bank, 5: air gap switch, 6: trigger pulse generator, 7: quartz or LiF window, 8: to pump.

The discharge circuit was the same for (*A*) and (*B*). The coaxial condenser bank of 1~2 μF, which was considerably larger than those reported,[9,10] was charged up to a voltage from 5 to 30 kV and the peak current amounted up to 30 kA. The period of the underdamped discharge current was 7 μs. The discharge current was observed with a Rogowski coil and the gap voltage with a potential divider for impulse voltage (Nichikon IVD-30K20P) on a synchroscope (Iwasaki DS-5305).

The *Z*-pinch laser tube was evacuated down to 3×10^{-5} Torr and gas was filled before each shot of discharge. Pure gases (99.99%) of O_2, N_2, Ne, Ar, Kr and Xe were used for the discharge. The pressure p_0 of the gas was measured with a thermocouple gauge, a cold cathode ion gauge and a thermal ion gauge, all of which were set near the gas inlet and calibrated beforehand with a Mcleod gauge.

It was difficult for us to adjust the internal mirror system in the vacuum. The alignment of the mirrors was worked out by using a He-Ne laser and movable diaphragms having a pinhole (see Fig. 1), which could be magnetically put into or away from the light path along the axis of the discharge tube.

The photographic and photoelectric observations of the laser oscillation lines were carried out with a GE-100 spectrograph, with a grating of 1200 lines per mm and 3000A blaze, in which a photographic plateholder and a two-channel photomultiplier unit were convertible. A condensing lens was not used between the entrance slit of the spectrograph and the front mirror of the *Z*-pinch laser. In the photographic observation the spectrograph was set sufficiently apart, about 1 m or so, from the front mirror and then the laser lines were photographed on a film (Fuji 3S or X-ray film) by one shot of discharge. When the spectrograph was set close to the front mirror, some spontaneous lines as well as laser lines were detected on the film, However, the spots on the film darkened by the spontaneous lines, shifted a little from those darkened spot of the laser lines, depending on the alignment of the cavity mirrors.

In the photoelectric observation, signals from photomultipliers (HTV 1P28 or R466) were displayed on a synchroscope (Iwasaki 5305 or Techtronics 485) by the trigger signal from the Rogowski coil which was induced by the initiation of discharge current. A proper value of the anode resister was selected for the photomultipliers depending on whether the peak height or the temporal profile of signals from the laser lines was measured. Signals from the laser lines were confirmed by the fact that when the rear mirror of the optical resonator was covered by the movable diaphragm, the signals from stimulated emissions disappeared.

In order to know the temporal sequence of several laser oscillations from different ions in the discharge of a given kind of gas, first the temporal profile of the signal from each laser line, and then the sum or difference of some pairs of signals from two lines were observed on a Techtronics 485 synchroscope. The temporal profile of the signal from the total laser light was also very useful to determine the temporal sequence and pressure dependence of laser oscillations. In addition to the temporal sequence, in order to know the initiation of laser oscillation, the signals of the discharge current and a strong laser light were several times traced on the two beam synchroscope, Iwasaki 5305, and the accuracy was ± 50 ns in the determination of the initiation time.

3. Results of Experiment

The observed oscillation lines from multiple ionized ions are listed in Table I, and in Fig. 2 are shown examples of ultraviolet spectra for the laser oscillations of O, Ne and Xe ions. The oscillation lines observed on a neutral atom are only NeI λ6145 and 5945 (λ in A), which are known as a super-radiance or self-termination laser line.[16,17] No molecular line was observed in the course of the experiment. The wavelengths of the observed oscillation lines are determined within the accuracy of ± 0.5 A and identified by ref. 18. Most of them are the lines so far observed on the usual ion laser in a capillary, but the OV λ2781.04 line has been first observed and identified as a four-valent ion laser line by the present authors.[14] As is shown on the spectrum of Fig. 3, Xe λ2316.53 line is at shorter wavelength than the NeIV λ2357.96 line.[18] The high efficiency green lines of XeIV λ4954 and 5956[20,21] were also observed with high power in the present Z-pinch discharge.

All of the oscillation lines listed in Table I were observed only at the first shot and not at the second or following shot of the discharge. The contamination of gas caused by the first shot discharge seemed to hinder the laser oscillation at the following shot. In general, in order to get the oscillation of a low gain transition on highly ionized ion, the complete evacuation of the Z-pinch tube down to the order of 10^{-5} Torr was necessary before the filling of test gas in the tube. However, the oscillation of the high gain transitions such as NIII λ4097 or ArII λ4765 and III λ3511 was insensitive to the

Table I. Observed laser lines in Z-pinch discharge.

Wavelength (Å)	Ion	Identification Upper-Lower
NITROGEN		
3478.76	N IV	$(^2S)3p\,^3P^o_2 - (^2S)3s\,^3S_1$
4097.32	N III	$(^1S)3p\,^2P^o_{3/2} - (^1S)3s\,^2S_{1/2}$
4103.38	N III	$(^1S)3p\,^2P^o_{1/2} - (^1S)3s\,^2S_{1/2}$
4630.55	N II	$(^2P^o)3p\,^3P^o_2 - (^2P^o)3s\,^3P^o_2$
OXYGEN		
2781.50±0.50*	O V	$(^2S)3p\,^3P^o_2 - (^2S)3s\,^3S_1$
2983.78	O III	$(^2P^o)3p\,^1D_2 - (^2P^o)3s\,^1P^o_1$
3047.13	O III	$(^2P^o)3p\,^3P_2 - (^2P^o)3s\,^3P^o_2$
3063.45	O IV	$(^1S)3p\,^2P^o_{3/2} - (^1S)3s\,^2S_{1/2}$
3385.54	O IV	$(^3P^o)3p\,^4D_{7/2} - (^3P^o)3s\,^4P^o_{5/2}$
3727.11±0.50*	O II	$(^3P)3p\,^4S^o_{3/2} - (^3P)3s\,^4P_{3/2}$
3749.49	O II	$(^3P)3p\,^4S^o_{3/2} - (^3P)3s\,^4P_{5/2}$
3759.88	O III	$(^2P^o)3p\,^3D_3 - (^2P^o)3s\,^3P^o_2$
4347.38	O II	$(^1D)3p\,^2D^o_{3/2} - (^1D)3s\,^2D_{3/2}$
NEON		
2357.96	Ne IV	$(^3P)3p\,^4D^o_{7/2} - (^3P)3s\,^4P_{5/2}$
2372.81±0.50*	Ne IV	$(^3P)3p\,^4D^o_{3/2} - (^3P)3s\,^4P_{3/2}$
2473.40	Ne III	...
2677.90	Ne III	$(^4S^o)3p\,^3P_{2,0} - (^4S^o)3s\,^3S^o_1$
2866.88	Ne ?	...
3319.75	Ne II	$(^1D)3p\,^2P_{1/2} - (^1D)3s\,^2D_{3/2}$
3323.74	Ne II	$(^3P)3p\,^2P^o_{3/2} - (^3P)3s\,^2P_{3/2}$
3345.55	Ne II	$(^1D)3p\,^2P^o_{3/2} - (^1D)3s\,^2D_{5/2}$
3378.30	Ne II	$(^3P)3p\,^2P^o_{1/2} - (^3P)3s\,^2P_{1/2}$
3393.2	Ne II	$(^3P)3d\,^2D_{3/2} - (^3P)3p\,^2D^o_{5/2}$
5944.83	Ne I	$3p'\left[\frac{3}{2}\right]_2 - 3s\left[\frac{3}{2}\right]^o_2$
6143.09	Ne I	$3p\left[\frac{3}{2}\right]_2 - 3s\left[\frac{3}{2}\right]^o_2$
ARGON		
2913.00	Ar IV	$(^3P)4p\,^2D^o_{5/2} - (^3P)4s\,^2P_{3/2}$
3002.66	Ar ?	...
3511.12	Ar III	$(^4S^o)4p\,^3P_2 - (^4S^o)4s\,^3S^o_1$
3637.89	Ar III	$(^2D^o)4p\,^1F_3 - (^2D^o)4s\,^1D^o_2$
4764.86	Ar II	$(^3P)4p\,^2P^o_{3/2} - (^3P)4s\,^2P_{1/2}$
KRYPTON		
2751.39	Kr ?	...
3049.70	Kr ?	...
3239.51	Kr III	$(^2P^o)5p\,^1D_2 - (^2P^o)5s\,^1P^o_1$

(Continued)

Wavelength (Å)	Ion	Identification Upper-Lower	
XENON			
2316.53±0.50*			
2527.11±0.50*			
2691.84	Xe III**?		···
3079.76	Xe III**?		···
3246.84	Xe III or IV**	$(^2P^o)6p\,^3D_3$	$-(^2D^o)5d\,^3D^o_3$
3306.04	Xe IV?		···
3330.90	Xe IV		···
3349.80	Xe IV**?		···
3454.24	Xe III	$(^2D^o)6p\,^1D_2$	$-(^2D^o)6s\,^1D^o_2$
3542.33	Xe III	$(^2D^o)6p\,^3P_2$	$-(^2D^o)6s\,^3D^o_3$
3645.51	Xe IV**?		···
3803.29	Xe IV**?		···
4060.41	Xe ?		···
4272.59	Xe III	$(^2D^o)6p\,^3F_4$	$-(^2D^o)5d\,^3D^o_3$
4305.75	Xe IV	$(^2D^o)6p\,^3D_3$	$-(^2D^o)5d\,^3D^o_3$
4954.18	Xe IV		···
5007.80	Xe IV		···
5260.17	Xe IV		···
5260.43	Xe II	$(^3P)6p\,^2P^o_{3/2}$	$-(^3P)6s\,^2P_{1/2}$
5352.90	Xe IV		···
5394.60	Xe IV		···
5955.67	Xe IV		···

* not observed in ref. 18
** identified by ref. 19

impurity content in N_2 or Ar gas, respectively. For example, the oscillation was observed for the NIII line even in the discharge of air, and for the Ar lines even in the mixture of Ar+N_2 with $p_0(Ar)=p_0(N_2)=5$ mTorr.

The pressure dependence of the peak height or intensity in the temporal trace of the signal from a laser line was observed for many oscillation lines of all gases tested. Figures 4(*a*) and (*b*) show the peak intensities of five laser lines of Ne in various ionization stages, and of all the observed lines of Ar, respectively, as a function of the initial filling gas pressure p_0. Figure 5 shows the peak intensity of multiple ionized N laser lines as a function of p_0. In each of the above figures, the relative intensity among the different laser lines has no meaning because the calibration was not performed on the spectral sensitivity distribution of the detecting system, including the spectrometer and photomultipliers.

Figure 6 shows the dependence of the optimum pressure of laser oscillation on the voltage of the condenser bank for three laser lines of Ar. As the voltage increases the optimum pressure shifts to a higher pressure for the ArIII λ3511 line and does a little

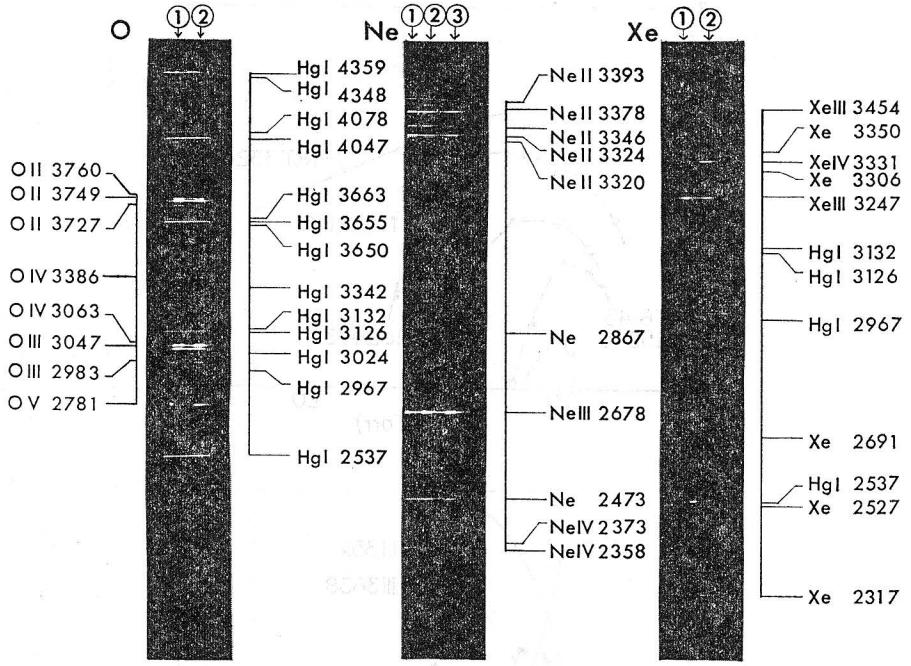

Fig. 2. Spectra of ultraviolet laser lines (C=2 μF, V=15 kV). O(1) p_0=5.0 and (2) 6.0 mTorr. Ne(1) p_0=8.0, (2) 9.0 and (3) 11.5 mTorr. Xe(1) p_0=3.0 and (2) 4.0 mTorr.

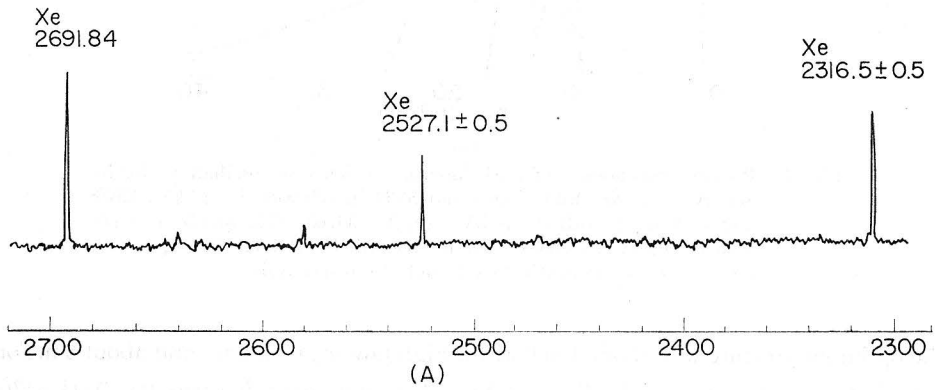

Fig. 3. Microphotometer trace of the spectrum of laser oascillations, Xe λ2316.5 and 2526.4 A.

for ArIII λ3638, while the optimum pressure shifts to a lower pressure for the ArII λ4765 line.

The optimum initial gas pressure for the laser oscillation was in the range from 5 to 20 mTorr for any laser line observed, namely 5∼10 mTorr for O_2 and N_2, 10∼20 mTorr for Ne and Ar, about 6 mTorr for Kr and 2∼4 mTorr for Xe. Further,

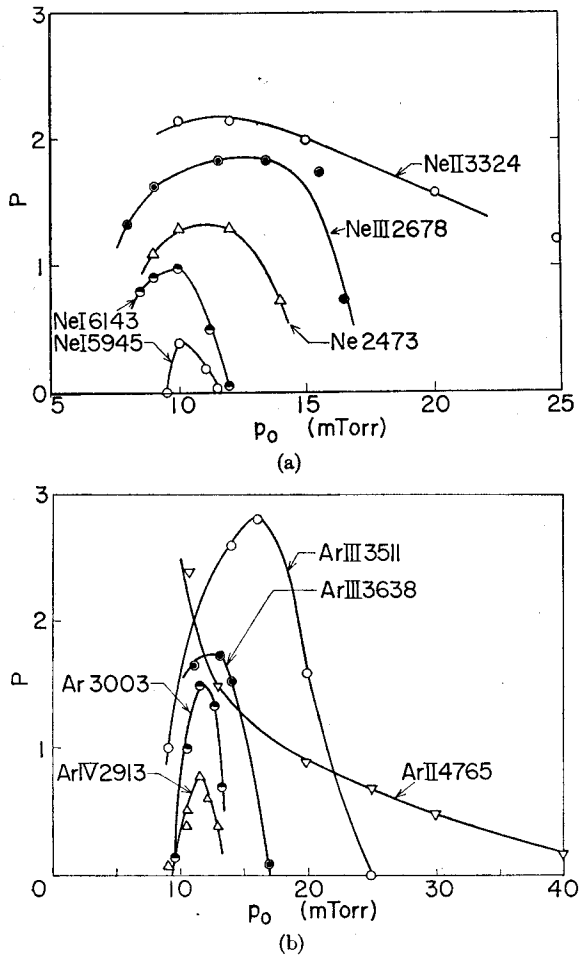

Fig. 4. Pressure dependence of peak intensity of ion laser oscillations for Ne and Ar. (*a*) Ne: λ6143, 5945 and 3324 in (*B*) with V=20 kV; λ2678 and 3324 in (*A*) with V=16 kV. (*b*) Ar: λ4765, 3511 and 3638 in (*B*) with V=13 kV; λ3003 and 2913 in (*A*) with V=12 kV. The apparatus (*A*) and (*B*) are indicated by (*A*) and (*B*), respectively.

the optimum pressure was about 4 mTorr for high power green lines and about 6 mTorr for all the observed ultraviolet lines of Xe. The only exception was the ArII λ4765 line. As is seen in Fig. 4(*b*), the optimum pressure of this line is very low, *i.e.*, lower than 10 mTorr, in contrast with those of the other oscillation lines of Ar.

Examples of the photo-electric signals from individual laser lines and the sum or difference of the two signals are shown in Figs. 7~10. Figure 7 shows each of the signals from the ArII λ4765, III λ3511, (?) λ3003 and IV λ2913 laser lines, where (?) means that the ionization stage to which the laser transition belongs is not known. Figures 8(*a*) and (*b*) show the sum of the signals from the Ar λ4765 and λ2913 lines and

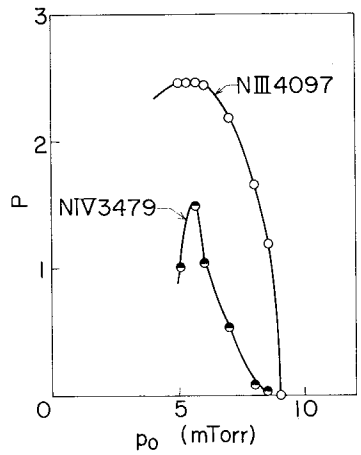

Fig. 5. Pressure dependence of peak intensity of N ion laser oscillations in (*A*) with V=23 kV. The initial pressure p_0 is given for N_2.

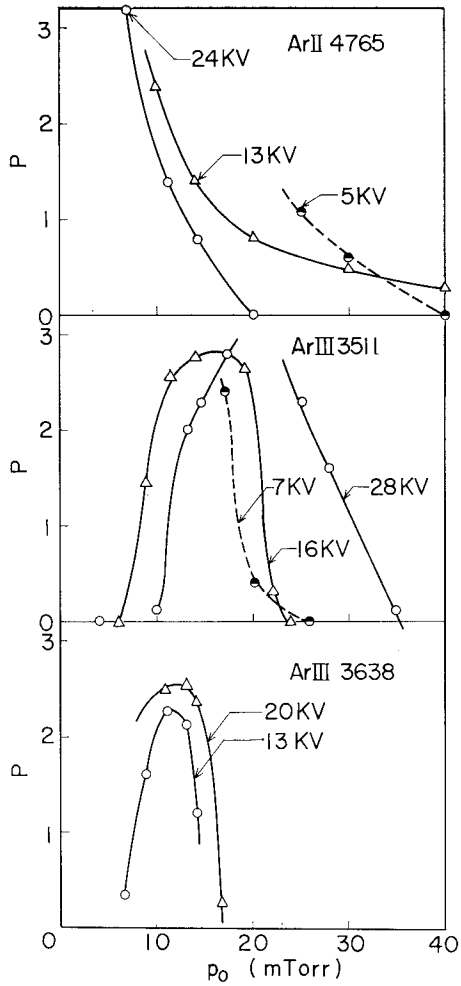

Fig. 6. Voltage dependence of peak intensities of ArII λ4765, III λ3511 and III λ3638 laser lines in (*A*).

that of the signals from the Ar λ3511 and 2913 lines, respectively. Figure 9 shows each of the signals from the Xe(?) λ2317, III λ3264 and IV 3331 lines. Figures 10(*a*) and (*b*) show the sum and difference of the signals from the Xe λ2317 and 3264 lines, respectively.

The temporal sequence of laser oscillations and its pressure dependence are shown for the observed Ar laser lines in Fig. 11, together with the temporal profiles of the discharge current and gap voltage of the discharge. In the present experiment, neither an abrupt change of the voltage nor kink of the current[9,22] at the pinch time of plasma were observed.[23] The pinch of plasma was ascertained by the observation of the continuum emission from the compressed plasma column, and the pinch time was determined by the simultaneous measurement of the discharge current and the total light

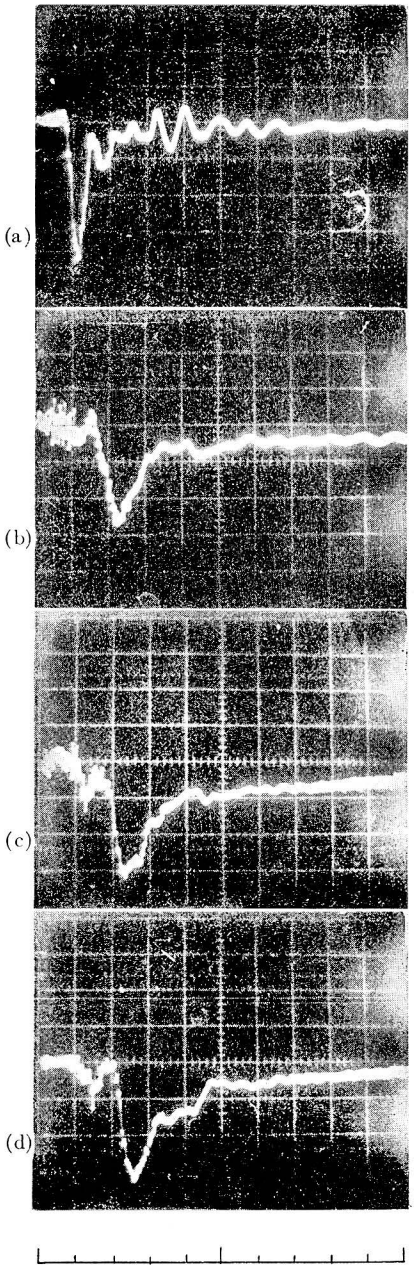

Fig. 7. Traces of oscillation pulses of Ar ion laser lines at p_0=10 mTorr for V=15 kV. (*a*) ArII λ4765, (*b*) ArIII λ3511, (*c*) Ar(?) λ 3003 and (*d*) ArIV λ2913. Time scale is in 50 ns/div.

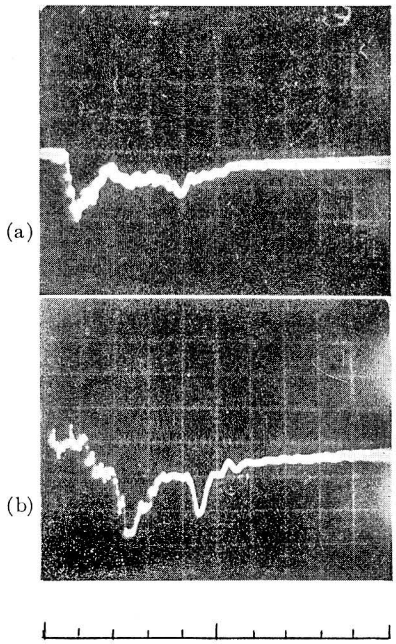

Fig. 8. The sum of two pulses of Ar ion laser lines at p_0=10 mTorr for V=11 kV; (a) the sum of ArII λ4765 (first pulse) and ArIV λ2913, (*b*) the sum of ArIII λ3511 and ArIV λ2913. Time scale is in 50 ns/div.

signal of the spontaneous emission from the discharge. The pinch time thus determined is 0.3～0.5 μs in the optimum gas pressure range (10～20 mTorr) for the laser oscillation of Ar. It is approximately equal to that of ref. 9, in which the discharge conditions are nearly the same as those of the present experiment.

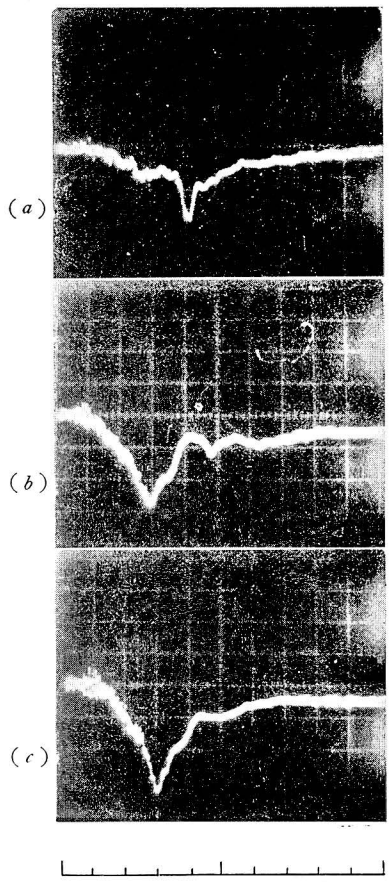

Fig. 9. Traces of oscillation pulses of Xe ion laser lines at $p_0=3$ mTorr for $V=15$ kV. (*a*) Xe(?) λ2317, (*b*) XeIII λ3264 and (*c*) XeIV λ3331. Time scale is in 50 ns/div.

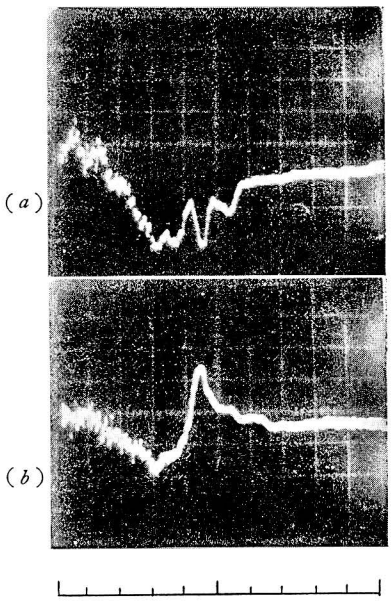

Fig. 10. The sum (*a*) and the difference (*b*) to two laser oscillation pulses, XeIII λ3264 (first pulse) and Xe (?) λ2317, at $p_0=3$ mTorr for $V=$ 15 kV. Time scale is in 50 ns/div.

From Fig. 11 it is seen that laser oscillations from different ionized species of Ar occur in the increasing order of the ionization stage, and that as the filling gas pressure increases, the laser oscillation from a higher ionized ion shows a larger time delay. The same results were also observed on the laser oscillations from O, N, Ne or Xe. Figure 12 shows the pressure dependence of the delay of the laser oscillation on the OV λ2781 line. The signal delays and becomes smaller as the pressure is increased from (a) 6.5 to (*c*) 7.5 mTorr. As is shown in Fig. 11, the oscillation time of the ArII λ4765 laser line does not change as the filling gas pressure is varied. This is also the exceptional behavior of the ArII λ4765 line together with the experimental results shown in Figs. 4(*b*) and 6.

The total energy emitted from the oscillation of the XeIV green laser lines (λ4954～

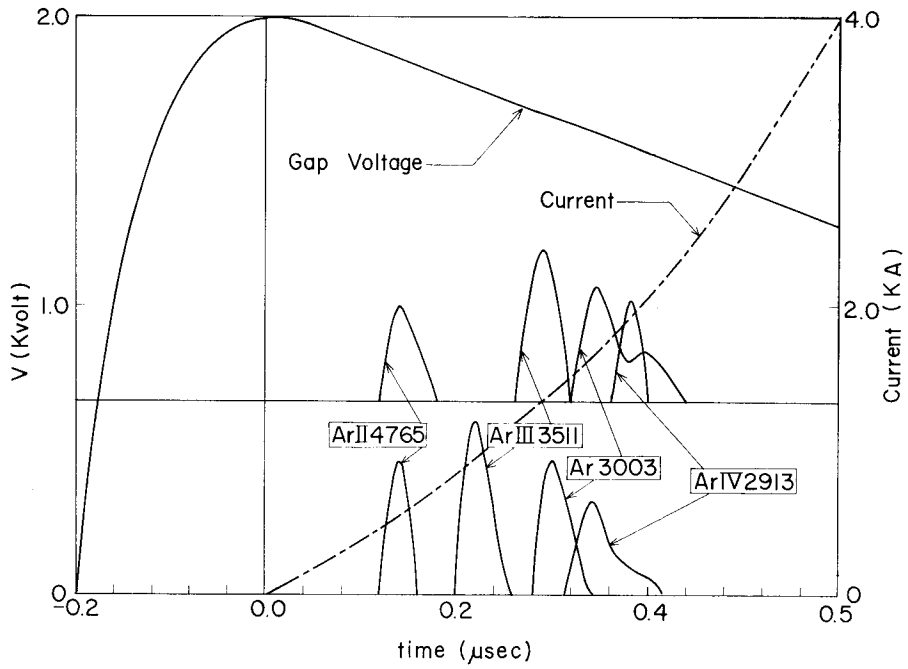

Fig. 11. The sketch of the train of Ar ion laser pulses, discharge current and gap voltage. The upper train at $p_0=12$ mTorr. The lower train at $p_0=9$ mTorr. The oscillation of ArIII λ3638 occurs at the same time as that of ArIII λ3511.

5956 in Table I)[8,20,21] was measured with a TRG Model 108 ballistic thermopile and Hewllet Packard 419A DC null voltmeter, when a dielectric-coated mirror ($R=2$ m) of 20% transmission was used in place of the front Al-mirror of the optical resonator in the apparatus (B). The energy was estimated to be 7×10^{-3} joule and hence the power amounted to 35 k watt from the observed average pulse width 0.2 μs of the oscilation.

4. Calculation and Ionization and Excitation

In order to understand the experimental results in §3, the calculations are made under the assumption of two different simple models for the ionization and excitation of plasma in the Z-pinch discharge. The first model is concerned with the ionization and excitation by thermal electrons for the successive laser oscillations from different ions during the plasma compression. The second model is concerned with the possibility of a direct excitation of the ArII λ4765 laser oscillation by high energy runaway electrons.[24~27]

4-1. Ionization during plasma compression

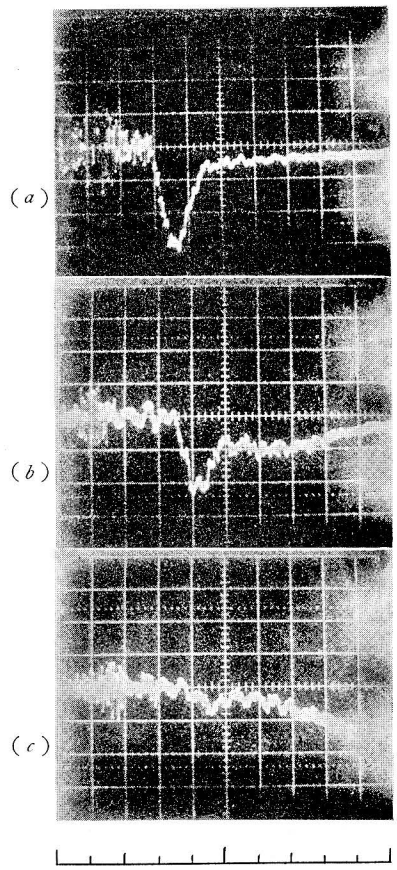

Fig. 12. Pressure dependence of laser oscillation pulse, OV λ2781 for V=15 kV. (*a*) p_0 =6.5, (*b*) 7.0 and (*c*) 7.5 mTorr.

The compression of plasma in the Z-pinch discharge was analyzed in the previous paper[23]; and the result gives a physical picture of plasma compression for the present calculation. A plasma of low ionization is uniformly formed in the Z-pinch tube immediately after the initial breakdown of gas discharge. Then, as the discharge current increases, it flows onto the surface of the plasma column due to the skin effect and the plasma column is adiabatically compressed by the magnetic field surrounding the column.

The calculation is performed on the rate equation for the ionization of Ar under the following assumptions: (i) all variables included in the equation are homogeneous over the cross section of the compressing plasma column; (ii) the role of excited states, especially of metastable states, is discarded in ionization; (iii) the electron velocity distribution is Maxwellian throughout the whole compression process of the plasma and (iv) no particle loss occurs from the plasma column during the compression. Then the rate equation is written as follows;

$$\frac{1}{n_e}\frac{\mathrm{d}n(i)}{\mathrm{d}t}=S(i-1,i)n(i-1)+\alpha(i+1,i)n(i+1)+\gamma(i+1,i)n_e n(i+1)$$
$$-S(i,i+1)n(i)-\alpha(i,i-1)n(i)-\gamma(i,i-1)n_e n(i)$$
$$-\frac{n(i)}{n_e}\frac{1}{\pi r(t)^2}\frac{\mathrm{d}}{\mathrm{d}t}\{\pi r(t)^2\} \quad \text{for } i=1,2,\cdots,7, \tag{1}$$

and

$$n_e=\sum_{i=1}^{7}(i-1)n(i), \tag{2}$$

where n_e is the number density of electrons, $n(i)$ is that of ions of i-species, $n(1)$ is that of neutral atoms and $r(t)$ is the radius of the compressing plasma column at a time t. Further, the rate coefficient for the electronic impact ionization from i to $(i+1)$-species is assumed to be given as [28]

$$S(i,i+1)=\frac{1.64\times10^{-6}}{U(i)T_e^{3/2}}\exp\{-U(i)\} \tag{3}$$

and the coefficient for the radiative recombination from $(i+1)$ to i-species by[28]

$$\alpha(i+1,i)=5.20\times10^{-14}(i+1)U(i)^{\frac{1}{2}}\times$$
$$\left\{0.429+\frac{1}{2}\ln U(i)+0.469/U(i)^{\frac{1}{2}}\right\} \tag{4}$$

with $U(i)=\chi(i,i+1)/T_e$, where $\chi(i,i+1)$ is the ionization potential of i-species in eV, and T_e is the electron temperature in eV. The rate coefficient for the three-body recombination from $(i+1)$ to i-species is easily obtained from eq. (3) by making use of the detailed balance.

The last term of eq. (1) corresponds to the change of particle density in the plasma column during the compression. The radius $r(t)$ of the plasma column should be solved as a function of time from the coupled equations of plasma motion and circuit of discharge as performed in the previous paper.[23] However, for simplicity, the following formula is assumed here for $r(t)$, referring to the results of experiment[10,30] and analysis;[23]

$$r(t)=\frac{r_0}{2}\left(1-\frac{r_p}{r_0}\right)\cos\left(\pi\frac{t}{t_p}\right)+\frac{r_0}{2}\left(1+\frac{r_p}{r_0}\right), \tag{5}$$

where r_0 is the radius of the discharge tube and r_p is that of the plasma column at pinch time t_p.

The temporal profile of the electron temperature $T_e(t)$ during the plasma compression should be determined in a consistent way with eqs. (1), (5) and the energy equation including radiation loss, but the problem is very complicated. Here, the following form of the profile $T_e(t)$ is assumed, referring to the numerical analysis by Düchs *et al.*[29] and the experimental result by Vasil'eva *et al.*[9] whose apparatus and discharge conditions are similar to those of the present experiment:

$$T_e(t)=(T_{em}-T_{e0})\left(\frac{t}{t_p}\right)^2+T_{e0} \quad \text{for} \quad 0\leq t\leq t_p,$$
$$(T_{em}-T_{e0})\left(\frac{t}{t_p}-2\right)^2+T_{e0} \quad \text{for} \quad t_p\leq t, \tag{6}$$

where $T_{em}=T$ at $t=t_p$ and $T_{e0}=T$ at $t=0$.

Corresponding to the plasma of low ionization formed immediately after the initial breakdown, the initial conditions are assumed as follows:

$$n(1)\neq 0, \quad n(2)/n(1)=0.1\sim 0.01, \quad n(3)=\cdots=n(7)=0 \quad \text{and}$$
$$T_{e0}=1\sim 2\,\text{eV} \quad \text{at} \quad t=0. \tag{7}$$

The computation has been carried out with FACOM 230-60 in Kyoto University for a combination of the values, $t_p=0.3$ or $0.5\,\mu$s, $r_p/r_0=0.1$ or 0.2 and $T_{em}=10$, 15 or 20 eV.

Figure 13 shows an example of the numerical solution of eq. (1) for $t_p=0.5\,\mu$s, $r_p/r_0=0.2$ and $T_{em}=15$ eV. Here, it is noticed that the number density $n(i)$ is expressed by $n(i)/n_{total}$ for $n_{total}=\sum_{i=1}^{7}n(i)$ and that the total number density n_{total} of heavy particles in the plasma column increases proportionally to $\{r_0/r(t)\}^2$ during the plasma compression. It is not possible for us to get any experimental or analytical proof for the initial condition (7), but the calculated result of the ionization process near the pinch time is insensitive to the values of $n(2)/n(1)$ and T_{e0} within the ranges assumed by the condition (7). The result is also hardly affected by a change in the

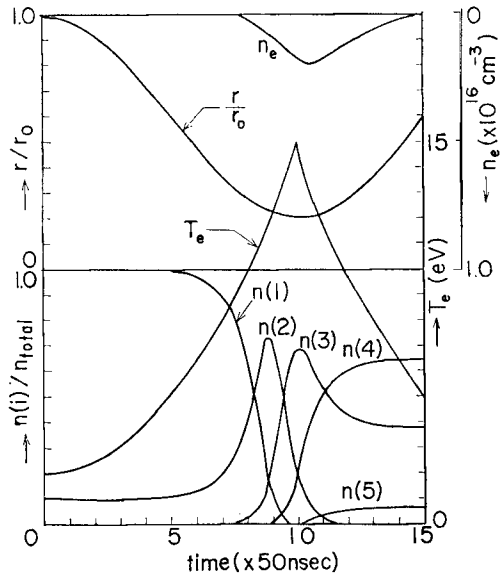

Fig. 13. The solution of eq. (1) for $t_p=0.5\,\mu$s, $r_p/r_0=0.2$ and $T_{em}=15$ eV. The functional from is depicted for T_e and r/r_0.

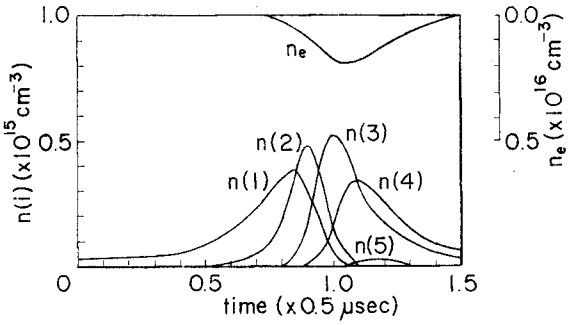

Fig. 14. The production of particles, n_e and $n(i)$, near the pinch time $t_p=0.5$ μs, which is calculated from the result of Fig. 13.

functional form of $T_e(t)$ and $r(t)$, but is much influenced by the change of the values of T_{em} and r_p.

The example of the solution in Fig. 13 leads to the temporal profiles of the particle densities, n_e and $n(i)$, during the plasma compression in Fig. 14. As will be discussed in detail in the next section, the productions of ions and electrons calculated are considered to be related to the experimental temporal sequence of Ar ion laser oscillations of Fig. 11, except for the oscillation of ArII the λ4765 line.

4-2. Excitation by runaway electrons

The electron runaway has been observed in the early nuclear fusion experiments[24~27], and the analysis has been given in some simple cases of fully ionized plasma.[31~36] The following calculation is performed on Ar plasma according to the simple method by Grossmann-Doearth,[26] in which the ionization ratio of plasma is taken into account and, for simplicity, the distributions of velocity and free path of runaway electrons are neglected.

The rate equation for the production of runaway electrons is given by

$$\frac{dn_R}{dt}=\bar{\varphi}-\frac{n_R}{\tau_R}, \tag{8}$$

and

$$\bar{\varphi}=\frac{W(\epsilon)}{\tau}(n_e-n_R)=\varphi(\epsilon)-\frac{W(\epsilon)}{\tau}n_R, \tag{9}$$

where n_R, τ_R and ϵ are the number density, life time and energy of the runaway electrons, respectively, n_e is the number density of the electrons in plasma and (n_e-n_R) is that of the thermal electrons.

Here, $W(\epsilon)$ is the probability for thermal electrons not to collide with any kind of particle until having reached an energy ϵ,

$$W(\epsilon)=\prod_i W_i(\epsilon), \tag{10}$$

and $W_i(\epsilon)$ is the probability for thermal electrons to travel a distances in the electric field E without being scattered by the i-th particle,

$$W_i(\epsilon)=\exp\left\{-\frac{n(i)}{E}\int_{\epsilon_{th}}^{\epsilon} q^i_h(\epsilon)\,d\epsilon\right\}, \tag{11}$$

with $\epsilon=eEs$, where $n(i)$ is the number density of the i-th particles and ϵ_{th} is the energy of the thermal electrons. The momentum transfer cross section $q^i_h(\epsilon)$ of the i-species of Ar is given by ref. 37 for the neutral atom ($k=0$) and by the formula of Drawin for $k\geq 1$.[38]

Further, $\bar{\varphi}(\epsilon)$ is the flux density of the runaway electrons reaching energy ϵ, and τ is the collision time of the thermal electrons, *i.e.*,

$$\frac{1}{\tau(v_{th})}=\sum_i \frac{1}{\tau_i(v_{th})}, \tag{12}$$

where $\tau_i(v_{th})$ is the collision time of the thermal electrons with the i-th particle and $v_{th}=60\sqrt{T_e(\text{in eV})}$ (cm/μs) is the velocity of the thermal electrons. The life time τ_R of the runaway electrons is approximately given by

$$\frac{1}{\tau_R}=\frac{1}{\tau_{R_1}}+\frac{1}{\tau_{R_2}}, \tag{13}$$

with $\tau_{R_1}=l/v_R(\epsilon)$ and $\tau_{R_2}=1/\{v_R(\epsilon).\ \sum_i n(i)q^i_h(\epsilon)\}$, where $v_R(\epsilon)=60\sqrt{\epsilon(\text{in eV})}$ (cm/μs) is the velocity of the runaway electrons of energy ϵ and τ_{R_1} and τ_{R_2} are the time for the runaway electrons to pass length l of the Z-pinch tube and the life time of the electrons determined by the collisions with the particles, respectively.

Equation (8) is transformed into

$$\frac{dn_R}{dt}=\varphi-\frac{n_R}{\bar{\tau}_R} \tag{14}$$

and

$$\frac{1}{\bar{\tau}_R}=\frac{1}{\tau'}+\frac{1}{\bar{\tau}_R}, \tag{15}$$

where $\tau'=\tau/W(\epsilon)$.

In the steady state we have $n_R=\bar{\tau}_R\varphi$ from eq. (14). Further, we have $n_R\simeq n_e$ for $\tau'\ll\tau_R$ and $n_R\simeq\tau_R\varphi$ for $\tau'\gg\tau_R$. In the latter case, if $\tau_R\simeq\tau$, then $n_R=n_eW(\epsilon)$.

In general, the solution of eq. (14) is given as

$$n_R(t)=\left(\int\varphi(t)e^{\tilde{\theta}(t)}\cdot dt+C\right)e^{-\tilde{\theta}(t)}, \tag{16}$$

where C is the constant of integration and

$$\varphi(t)=\frac{1}{\tau(t)}W(t)\ n_e \text{ and } \tilde{\theta}(t)=\int\frac{dt}{\bar{\tau}_R(t)}.$$

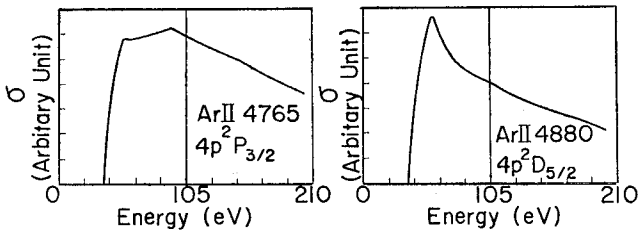

Fig. 15. Direct excitation cross sections for the upper levels of ArII λ4765 and 4880. $\sigma_{max}(4765)=1.0\times10^{-18}$ cm² and $\sigma_{max}(4880)=0.8\times10^{-18}$ cm².

As is shown in Fig. 15,[37] the cross section σ for the direct excitation[38,39] by an electron collision from the ground state of ArI to the upper level $4p^2P_{3/2}$ of the ArII λ4765 laser transition is larger than that to the upper level $4p^2D_{5/2}$ of the ArII λ4880 laser transition in a range of electron energy higher than 80 eV. In connection with the experimental fact that the laser oscillation of the Ar λ4880 line was not observed in contrast to the strong emission of the Ar λ4765 laser line in the Z-pinch discharge, it is probable that runaway electrons having energy higher than 80 eV effectively excite the laser oscillation of the Ar λ4765 line.

Here, we try to calculate the time dependent solution, $n_R(t)$ with energy $\epsilon=100$ eV, of eq. (16) in the electric field of $E=20$ V/cm for the temporal profiles of particle densities and electron temperature, n_e, $n(i)$ and T_e, in Figs. 13 and 14. Figure 16 shows the temporal profile of the density of runaway electrons $n_R(t)$ together with the product of $n_R n(1)$. The decrease of $n_R(t)$ at about 250 ns after the breakdown is mainly due to the increase in stopping power resulting from the increase of a heavy particle density in the plasma column. The absolute value of the maximum n_R somewhat exceeds the value of electron density corresponding to the maximum current of the discharge, but this is due to the crude model and initial condition of the present treat-

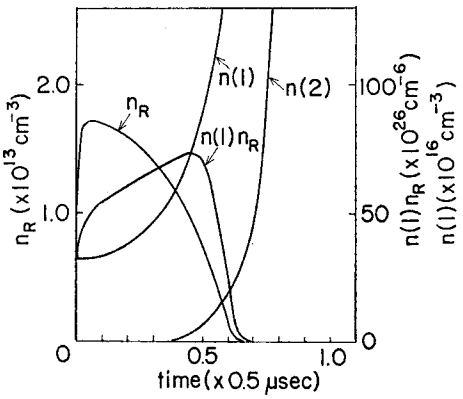

Fig. 16. The temporal profile of runaway electron density n_R and the product n_R $n(1)$ for the production of particles in Fig. 14.

ment. The value $n_R n(1) v_R \sigma$ gives the rate of the direct excitation to the laser upper level. Hence, Fig. 16 indicates that the laser oscillation excited by the runaway electrons is apt to occur at a very early time, not later than half of the pinch time, after the initial breakdown of the discharge. Detailed discussions will be given in the next section.

5. Discussion

The calculation of 4-1 gives the successive production of ions near the pinch time t_p in the increasing order of the ionization stage during the plasma compression as shown by $t_p=0.5$ μs in Fig. 14. In the experiment, the train of successive laser oscillation pulses (pulse width of about 50 ns) appears from different ions in the increasing order of ionization for the discharges of all kinds of gases tested. Fig. 11 shows the train of oscillation pulses from Ar ions for the filling gas pressure p_0 of about 10 mTorr. In this figure, the time t_p is estimated from the value of p_0 by making use of the analysis in the previous paper[23] because it was difficult to get a definite value of t_p in the experiment. Further, in the experiment, for all the observed Ar laser lines, except the ArII λ4765 line, the optimum gas pressure for the laser oscillation is in the range from $p_0=10$ to 20 mTorr (Figs. 4(*b*) and 6), which corresponds to the time range from 0.3 to 0.5 μs, respectively.[23] The oscillation time of these lines was delayed as the pressure p_0 was increased (see Figs. 11 and 12). Only the ArII λ4765 line showed the anomalous behavior of oscillation. The optimum gas pressure of this line for the laser oscillation is very low, *i.e.*, lower than 10 mTorr (Fig. 4(*b*) and 6) and the oscillation time hardly changed by increasing pressure p_0.

From the correspondence between the calculated temporal sequence of ion production and the observed temporal sequence of laser oscillations it is considered that the ArIII λ3638 and 3511, Ar(?) λ3003 and ArIV λ2913 laser lines are excited from the ions produced near the pinch time by the plasma compression. Further, if the correspondence is assumed between the laser oscillations from ArII to ArIV in Fig. 11, and the production of ions $n(i)$ in Fig. 14 by taking account of the intervals of their temporal successions, it is probable that the upper levels of the ArIII λ3511 and 3638 laser lines are excited from the ArII ions, $n(2)$ in Fig. 14. The ArIV λ2913 line is probably excited from the ArIII ions, $n(3)$ in Fig. 14, and possibly the Ar(?) λ3003 line is also excited from the ArIII ions through the step-by-step[40,31] or direct [48,39] excitation process by thermal electrons of $T_e=10\sim20$ eV. The excitation from the neutral particles, $n(1)$ in Fig. 14, does not occur because of a low electron density and the temperature of the plasma column.

As is described above, the anomalous low value of optimum gas pressure and the very early time of oscillation for the ArII λ4765 line indicates the possibility that this

laser line is excited by high energy runaway electrons. The result of the calculation of §4-2 also shows the possibility that the oscillation of the ArII λ4765 line takes place very early, not later than a half of the pinch time t , after the initial breakdown of the discharge. The increase of heavy particle density prevents runaway electrons from remaining in the plasma column. The pressure range of $p_0=10\sim20$ mTorr, which is optimum for the laser oscillation of the observed Ar ion lines, except for the ArII λ4765 line, corresponds to the range of pinch time, $t_p=0.3\sim0.5$. Therefore, the result of the calculation explains the experimental result that the oscillation time of the 4765 line is insensitive to the variation of p_0 in the above range.

In order to make clear the excitation mechanism of laser oscillations in the Z-pinch discharge, further experiment is necessary to perform more accurate measurements with a higher sensitivity and time resolution. In the above discussions, for example, it is not clear why the laser oscillation of the ArII λ4880 or 4765 line is not excited by thermal electrons during the plasma compression. A high value of E/p_0 gives rise to stronger emission from the ArII λ4765 line than from the ArII λ4880 line. Latimer and St. Johns' criterion suggests that the former line has a higher power than the latter under the Maxwell velocity distribution of electrons of $T_e=20$ eV.[37] Even if these criteria are applied to the present case, the possibility still remains that either of the laser lines may be excited from the particles, $n(1)$ and $n(2)$ in Fig. 14, by thermal electrons during the plasma compression.

In the observation of laser oscillations in the ultraviolet region it is a problem how to assign an observed line to some ionization stage or to some known transition. The time sequence of ion laser oscillations in the increasing order of ionization stage seems to be useful to know the ionization stage to which an observed line belongs. For examples, the Ar(?) 3003 line may be assigned to ArIV as seen in Fig. 11, and Xe(?)

Table II. Isoelectronic transitions*

$(^2P^o)3p^3P_2$	— $(^2P^o)3s^3P^o_2$			
CI	NII^{++}	OIII^{++}	FIV	NeV
9094.83	4630.55	3047.13	2298.29	1818±20 (in vac.)
$(^1S)3p^2P^o_{3/2}$	— $(^1S)3s^2S_{1/2}$			
CII	NIII^{+}	OIV^{+}	FV	NeVI
6578.05	4097.32	3063.45	2450.63	2042.38
$(^2S)3p^3P^o_2$	— $(^2S)3s^3S_1$			
CIII**	NIV^{++}	OV^{+}	FVI	NeVII
4647.45	3478.76	2781.50	2315.39	1981.98 (in vac.)

* wavelength in air, ** laser line listed in ref. 18, $^{+}$ and $^{++}$ laser lines observed in Z-pinch discharge, $^{++}$ strong lines.

λ2371 may belong to XeIV from Fig. 10. In order to assign a laser line to some electronic transition, the isoelectronic sequence of transitions is very useful. Table II shows the sequence of transitions: $(^2P^o)3p^3P_2$—$(^2P^o)3s^3P^o_2$, $(^1S)3p^2P^o_{3/2}$—$(^1S)3s^2S_{1/2}$ and $(^2S)3p^3P^o_2$—$(^2S)3s^3S_1$. The wavelength of the transitions in the table is given in refs. 42 and 43, except for the NeV transition. Several transitions among them have been observed as a laser line in the *Z*-pinch discharge. The laser line of OV λ2781 has been first observed by the present authors.[15] The wavelength and transition of NeV, which are unknown at present, are determined by applying the empirical relation[44,45] to the series from CI to FIV.

The laser oscillation of the NeV∼VII transitions are expected to occur in the vacuum ultraviolet region and a preliminary observation is being carried out with a SGV-50 Seya-Namioka monochromator joined to the *Z*-pinch laser tube.

Acknowledgements

This work was partly supported by Grant-in Aid of the Ministry of Education. One of the authors (Y.H.) is supported by the Fellowship of Japan Society for the Promotion of Science.

References

1) W. R. Benett, Jr.: Appl. Optics suppl II. Chemical Lasers (1965).
2) W. Demtröder and E. Elendt: Z. Naturforsch. **21a**, 2047 (1966).
3) G. R. Levinson, V. F. Papulovskiy and V. P. Tychinskiy: Radio Engng. and Elec. Phys. **13**, 4 (1968).
4) S. Hattori and T. Goto: Japan J. appl. Phys. **8**, 1159 (1969).
5) S. G. Kulagin, V. M. Likhachev, E. V. Markuzon, M. S. Rabinovich and V. M. Stovskii: JETP Letters **3**, 6 (1967).
6) V. M. Likhachev, M. S. Rabinovich and V. M. Sutovskii: JETP Letters **5**, 43 (1967).
7) V. M. Likhachev, M. S. Rabinovich and V. M. Sutovskii: *Eighth International Conference on Ionization Phenomena in Gases,* Vienna (1967) p. 259.
8) A. Papayanou and I. Gumeiner: Appl. Phys. Letters **16**, 5 (1970).
9) A. N. Vasil'eva, V. M. Likhachev and V. M. Sutovskii: Soviet Physics-Technical Physics **14**, 246 (1969).
10) R. Illingworth: J. Phys. D. appl. Phys. **3**, 924 (1970).
11) J. S. Hitt and W. T. Haswell: IEEE J. Quant. Electronics **QE-2**, xlii (1966).
12) P. K. Cheo and H. G. Cooper: J. appl. Phys. **36**, 1862 (1964).
13) W. B. Bridges and N. A. N. Chester: Appl. Optics **4**, 573 (1965).
14) Y. Hashino, K. Katsuyama and K. Fukuda: Japan J. appl. Phys. **12**, 470 (1972).
15) Y. Hashino, Y. Katsuyama and K. Fukuda: Japan. J. appl. Phys. **11**, 907 (1972).
16) D. C. Clunie, R. S. A. Thorn and K. E. Frezise: Phys. Letters **14**, 28 (1965).
17) D. Rosenberger: Phys. Letters **13**, 228 (1964).
18) W. B. Bridges and A. N. Chester: *Handbook of Lasers* (CRC, Ohio, 1971) p. 907.
19) E. Gallego Lluesma, A. A. Tagliaferri, C. A. Massone, M Gravaglia and M. Gellardo: J. Opt. Soc. Am. **63**, 362 (1973).

20) W. W. Simins and R. S. White: IEEE J. Quant. Electronics **QE–6**, 446 (1970).
21) W. R. Bridges, A. N. Chester, A. S. Halsted and J. V. Parker: Proc. IEEE **59**, 724 (1971).
22) Von U. Grossmann-Doearthe: Z. Naturforschg. **16a**, 1290 (1961).
23) Y. Hashino, H. Suemitsu and K. Fukuda: Japan. J. appl. Phys. **11**, 710 (1972).
24) Von E. Fünter, G. Lehner and H. Tuczek: Z. Naturforschg. **15a**, 566 (1960).
25) A. Gibson and D. W. Mason: Proc. Phys. Soc. **79**, 326 (1960).
26) Von U. Grossmann-Doearth: Nuclear Fusion, Suppl. part 3 (1962) 1007.
27) H. De Kluvier and T. Kawamura: Phys. Fluids **9**, 2715 (1967).
28) A. C. Kolb and R. W. McWhirter: Phys. Fluids **7**, 519 (1964).
29) D. Düchs and H. R. Griem: Phys. Fluids **9**, 1099 (1966).
30) K. Ishii, H. Suemitsu and K. Fukuda: Japan. J. appl. Phys. **5**, 1235 (1966).
31) A. V. Gurevich: Soviet Phys. JETP **12**, 904 (1961); **11**, 85 (1960); **11**, 1150 (1960).
32) H. Dreicer: Phys. Rev. **115**, 238 (1959); **117**, 329 (1960); **117**, 343 (1960).
33) F. C. Field: Phys. Fluids **7**, 1937 (1964).
34) M. D. Kruskal and I. B. Bernstein: Phys. Fluids **7**, 407 (1964).
35) D. V. Sivukhin: *Reviews of Plasma Physics*, ed. M. A Leontovich, vol. 4 (Consultants Bureau, New York, 1966) p. 153.
36) I. P. Shkarofsky, T. W. Johnston and M. P. Bachynski: *The Particle Kinetics of Plasma* (Addison-Wesley, 1966) p. 400.
37) I. D. Latimer and R. M. St. John: Phys. Rev. **A1**, 1612 (1970).
38) P. R. Cheo and H. G. Cooper: J. appl. Phys. **36**, 1862 (1965).
39) W. R. Benentt, Jr., J. W. Knutson, Jr., G. N. Mercer and J. L. Detch: Appl. Phys. Letters **4**, 180 (1964).
40) W. B. Bridges and A. N. Chester: Appl. Optics **4**, 573 (1965).
41) E. I. Gordon, E. E. Labuda and R. C. Miller: IEEE J. Quantum Electronics **QE–1**, 273 (1965).
42) C. E. Moore: *Atomic Energy Levels*, vol. I (NBS, 1949).
43) A. P. Striganov and N. S. Sventitskii: *Tablitsi Spektral'nikh Linii, Neitral'nykh i Ionizovannykh* (Atomizdat, Moskva, 1966).
44) A. E. Goertz: J. Opt. Soc. Am. **55**, 742 (1965).
45) R. Akerib: J. Opt. Soc. Am. **53**, 918 (1963).